PCCP

PAPER

View Article Online
View Journal | View Issue

Cite this: *Phys. Chem. Chem. Phys.*, 2014, **16**, 24800

The effect of the reactant internal excitation on the dynamics of the $C^+ + H_2$ reaction

D. Herráez-Aguilar,[a] P. G. Jambrina,[a] M. Menéndez,[a] J. Aldegunde,[b] R. Warmbier[c] and F. J. Aoiz*[a]

Received 24th July 2014,
Accepted 8th September 2014

DOI: 10.1039/c4cp03289f

www.rsc.org/pccp

We have performed a dynamical study of the endothermic and barrierless $C^+ + H_2(^1\Sigma_g^+) \rightarrow CH^+(^1\Sigma_g^+) + H$ reaction for different initial rotational states of the $H_2(v = 0)$ and $H_2(v = 1)$ manifolds. The calculations have been carried out using quasiclassical trajectories and the Gaussian binning methodology on a recent potential energy surface [R. Warmbier and R. Schneider, *Phys. Chem. Chem. Phys.*, 2011, **13**, 10285]. Both state-selected integral cross sections as a function of the collision energy and rate coefficients, $k_{v,j}(T)$, have been determined. We show that rotational excitation of the reactants is as effective as vibrational excitation when it comes to increasing the reactivity, and that both types of excitation could contribute to explain the unexpectedly high abundance of CH^+ in the interstellar media. Such an increase in reactivity takes place by suppressing the reaction threshold when the internal energy is sufficient to overcome the endothermicity. Whenever this is the case, the excitation functions at collision energies $E_{coll} \leq 0.1$ eV display a $\propto E_{coll}^{-1/2}$ dependence. However, the absolute values of the state selected $k_{v=1}(T)$ are one order of magnitude below the Langevin model predictions. The disagreement between the approximately derived experimental rate coefficients for $v = 1$ and those calculated by this and previous theoretical treatments is due to the neglect of the effect of the rotational excitation in the derivation of the former. In spite of the deep well present in the potential energy surface, the reaction does not show a statistical behaviour.

1 Introduction

The reaction of $C^+ + H_2(^1\Sigma_g^+)$ to form the methylidyne cation and one hydrogen atom has been extensively studied due to its particular features[1–3] and to its relevance for different scientific areas. In principle, from the electronic point of view, it could be expected to be one of the simplest triatomic processes, involving just five valence electrons, one of them of p nature, and hence presumably liable to accurate electronic structure treatment. However, the concurrence of several electronic states and the resulting avoided crossings complicate those calculations considerably. In addition, this reaction also constitutes a prototype of endothermic ($\Delta H_0^o \approx 0.40$ eV) ion–molecule reaction mediated by the presence of a well of $\approx$4.3 eV depth with respect to the $C^+ + H_2$ asymptote. Apart from that, the potential is essentially barrierless favouring the insertion approach and, consequently, the $C^+ + H_2$ reaction is a good candidate to test various statistical methods. Since the discovery of the methylidyne cation in the diffuse interstellar medium,[4] this reaction and its reverse have been the subject of a great deal of attention by astrophysicists since it was not straightforward to explain the high abundance of CH^+ under conditions of low temperature, considering its high reactivity and its likely slow formation due to the endothermicity of the direct reaction.

From the experimental point of view, the study of the title reaction has suffered from difficulties due to the high reactivity of the CH^+ product. Most of the experimental data for the abstraction reaction are several decades old. First studies[1,2,5,6] focused on the determination of the reaction threshold and the excitation function (translational energy dependence of the total integral cross section) both for the reaction with H_2 and for its deuterated isotopic variants. The results evinced how, for low collision energies, the reaction takes place through complex formation, with a threshold energy which nearly coincides with the endothermicity and a maximum value of the excitation function close to 2–3 Å^2. Angular distributions of CH^+ products were also determined as a function of the collision energy.[6–8] Such distributions displayed an almost isotropic distribution at energies up to approximately 4 eV, apparently indicating that the process takes place through formation of a complex characterized by a lifetime exceeding the rotational period of the system. At higher energies, however, the angular distributions became no longer isotropic.

[a] *Departamento de Química Fsica I, Facultad de CC. Químicas, Universidad Complutense de Madrid, 28040 Madrid, Spain. E-mail: aoiz@quim.ucm.es*
[b] *Departamento de Química Física, Facultad de Química, Universidad de Salamanca, 37008, Spain*
[c] *Materials for Energy Research Group and DST-NRF Centre of Excellence in Strong Materials, School of Physics, University of the Witwatersrand, Private Bag 3, 2050 Johannesburg, South Africa*

Ervin and Armentrout carried out detailed guided ion beam experiments[1,2] measuring the total cross section in a wide range of collision energies with special attention to the threshold region. In parallel, Gerlich and co-workers[9] carried out both experiments and phase space theory calculations (PST) in order to study the rotational dependence of the title reaction. Their results predict that rotational excitation of the H_2 molecule enhances the excitation function and the rate coefficient by lowering the effective barrier to reaction. In 1997, Hierl and collaborators[10] used a high temperature flowing afterglow apparatus to measure the thermal rate constants in the range of 400–1300 K for the $C^+ + H_2$ and $C^+ + D_2$ reactions. The value of the activation energy obtained from the temperature dependence of the thermal rate coefficients coincided almost exactly with the endothermicity, indicating that there is no energy barrier to the reaction in addition to the endothermicity. They found that the rotational and translational energies are equally effective when it comes to surmounting the reaction barrier. From their results, they also infer that the H_2 vibrational excitation was particularly effective from this point of view and lead to a significant increase of the reactivity. Using their thermal $k(T)$ for the reaction at high temperatures, they approximately derived rate coefficient values for the reaction with $H_2(v = 1)$ of $1–2 \times 10^{-9}$ cm^3 s^{-1}, a value very close to the Langevin collision rate coefficient, which represents an enhancement of $\approx 10^3$ with respect to the $v = 0$ thermal rates.

The first theoretical studies were performed by Truhlar,[11] who applied the PST to the reaction in order to describe the energy dependence of the cross section. Later on other authors[3,9] used experimental data to improve the PST calculations. Before summing up other dynamical studies performed for this system, it is worth mentioning that several potential energy surfaces have been developed over time. In 1977, Herbst[12] obtained a fitted PES for the $^2A'$ ground state and integrated quasi-classical trajectories (QCT) based on that potential.[13] González *et al.* also used QCT on a modified LEPS PES to study this reaction in the vicinity of the threshold. Aiming to study the photodissociation of the metastable CH_2^+ ion, Galloy *et al.*[14] performed an *ab initio* study of the excited states of the cation in 1978. Some years later, Jaquet and Staemmler[15] obtained a PES at a CEPA-PNO level for both the collinear and perpendicular abstraction reactions between the $C^+(^2P)$ cation and the ground H_2 molecule. That same year, Sakai *et al.*[16] carried out calculations for the potential energy surfaces of the six low lying states of the reaction $C^+ + H_2$ with an *ab initio* MCSCF-POLCI method. In 2005, Stoecklin and Halvick[17] published an analytical fit of a grid of 3291 high level *ab initio* points (hereinafter, SH PES) corresponding to the ground state of the CH_2^+ system and they used it to determine the rate constants for the reverse $H + CH^+$ reaction using the RIOSA (reactive infinite order sudden approximation with negative imaginary potential) QM approximate treatment. They concluded that the Langevin model overestimates the rate constants as a result of the two barriers in collinear approaches (C–H–H and H–C–H) of the CH_2^+ system. Subsequently, PST and QCT calculations have been performed on this surface, especially for the reverse reaction.[18] More recently, Zanchet *et al.*[19] carried out extensive accurate time dependent wave packet calculations (TDWP) on the SH PES, in order to determine the excitation functions and rate coefficients of the $C^+ + H_2(v = 1, j = 0–1)$ reaction. In 2011 Warmbier and Schneider[20] presented a new ground state potential energy surface for the CH_2^+ system. They used the highly accurate *ab initio* MRCI method and the aug-cc-pVTZ basis set to calculate as many as 16 259 *ab initio* points. Those points were then used to produced a PES fit based on high-order polynomials with special corrections taking into account the avoided crossing at and near the linear configurations. The resulting analytical PES (hereinafter WS PES) is then supposed to be most accurate for this reaction system. This PES was used by these authors to perform QCT calculations for the reverse reaction. The WS PES has been used in the present study.

The dynamics of the CH_2^+ system has drawn a great deal of attention by astrophysicists, since CH^+ was the first cation ever identified in the interstellar space by Douglas and Herzberg in 1941.[21] As commented on above, however, the mechanism of formation and destruction of this species was unclear. The problem stems from the unexpectedly high abundance[22] of a molecule as reactive as CH^+, which can only be explained through an efficient production mechanism that offsets its fast destruction. Recent publications[23] suggested that such a mechanism could be somehow related to collisions involving vibrationally excited H_2 molecules present in the interstellar medium. In this context, the reaction between C^+ and H_2 molecules vibrationally excited by far-UV fluorescence is the most obvious candidate to explain the CH^+ abundance.[22,23]

As mentioned above, Zanchet *et al.*[19] carried out TDWP quantum scattering calculations for the title reaction on the SH PES. Their cross sections were $\approx 30\%$ lower than those estimated by the experimental/theoretical study reported by Gerlich *et al.*[9] which included the participation of higher H_2 rotational states. In addition, the rate coefficients for the $C^+ + H_2(v = 1, j = 0, 1)$ reaction were found to be about a factor of 6 lower than the rough estimation made by Hierl *et al.*,[10] subject, in turn, to an uncertainty no less than a factor of two. Inserting the values calculated on the SH PES into the chemical codes, it was estimated that the amount of CH^+ would decrease by 30% in the diffuse interstellar medium. Moreover, it was concluded that the formation of CH^+ in the diffuse gas predominantly occurs through reaction with H_2 in $v = 0$ although, presumably, with rotational excitation.[19] The repercussion of the calculated rate coefficients on the amount of CH^+ in the hot and dense protoplanetary disks was found to be even more substantial, leading to a reduction by a factor of five, although the estimation relies on the existing values of the destruction state specific rates *via* the reverse reactions.[19] On the other hand, when the computed state-to-state rate coefficients were incorporated in a radiative transfer model code applied to the conditions of the Orion Bar photodissociation region, it was found that they have a considerable impact on the rotational distribution of the CH^+ cation affecting most especially the high rotational states whose transition fluxes were increased by up to 20% partly explaining the discrepancy between the observed and modeled results.

Zanchet *et al.*[19] concluded their work by pointing out the necessity of accurate calculations for higher rovibrational states of reactants, which is precisely one of the goals of the present article: to analyze the effect of rotational excitation of the hydrogen molecule on the rate constants of the $C^+ + H_2$ reaction and compare them with those obtained with vibrational excitation. To this end, we have used the QCT method which has been shown[24] to be fairly accurate for the description of insertion reactions, even at collision energies of the order of 10^{-3} eV. As already commented on, present calculations have been carried out on the WS PES,[20] which is presumed to be more accurate than previous PESs and predicts an endoergicity somewhat closer to, although slightly higher than, the experimental value. In addition, the unbiased statistical QCT method[25,26] has been also tested to discern to what extent the direct reaction is amenable of a statistical treatment.

The article is organized as follows: Section 2 briefly describes the theoretical methods that are used in the scattering calculations whose results are presented, discussed and analyzed in Section 3. Finally, Section 4 sums up the main conclusions drawn from such analysis.

2 Theoretical methods

In the interaction between a C^+ atom and a ground state H_2 molecule, there are three possible electronic states, labeled $1^2A'$, $1^2A''$ and $2^2A'$ in the C_S symmetry. Only the $1^2A'$ surface correlates the ground state $^2P_{1/2}$ of reactants with the ground state of products $H(^2S) + CH^+(^1\Sigma)$ throughout the CH_2^+ complex in the $^2A_1$ state in the C_{2v} symmetry. The $1^2A''$ and $2^2A'$ surfaces connect the excited spin–orbit $^2P_{3/2}$ ground state of C^+ with the excited state of products $H(^2S) + CH^+(^3\Pi)$, corresponding, respectively, to the electronic $^2B_1$ and $^2B_2$ states of the C_{2v} complex.

Our calculations have been carried out on the WS PES.[20] Table 1 displays the difference between the dissociation energies of the products and reactants, the reaction enthalpy at 0 K, the zero point energies of the H_2 and the methylidyne cation, and the depth well with respect to the reactant's asymptote. For comparison purposes, the corresponding values of the alternative SH PES[17] are also shown in Table 1. Although the agreement between both surfaces is reasonably good, some significant differences exist in the values of the reaction endothermicity (ΔD_e and ΔH_0^o). Both PESs feature the existence of a very deep well (more than 4 eV from the $C^+ + H_2$ asymptote) corresponding to the formation of the methylene cation which displays an angular geometry (H–$\widehat{C}$–H angle 141.2° in the WS PES). In addition, they lack any barrier in the entrance and exit valleys for the insertion approach. The sketch of the minimum energy path is shown in Fig. 1. As it becomes evident from the analysis of this curve, the path presents a local maximum in the vicinity of the entrance valley whose cusp is located below both asymptotes followed by the aforementioned well. The geometry associated with each of the points of the curve that connect the reactant asymptote with the absolute minimum corresponds to that of an insertion reaction; *i.e.*, the C^+ atom preferably approaches the hydrogen molecule following a T-geometry so that it causes the H–H bond to stretch and, finally, it inserts itself between both hydrogen atoms. All these features would lead to expect, at least at first instance, a statistical behaviour and hence it would be pertinent to test the results derived with a rigorous statistical model.

Table 1 Relevant data of the energetics for the CH_2^+ system. The differences between the product and reactant dissociation energies referred to their respective potential asymptotic minimum, $\Delta D_e = D_e(CH_2^+) - D_e(H_2)$, are shown in the first row. All the results are in eV and the well depth is referred to the reactant asymptote. In the present work, the WS PES has been used for all the calculations[20]

Property	WS[20]	SH[17]	Exp.
ΔD_e	−0.518	−0.468	−0.496[20]
ΔH_0^o	0.424	0.373	0.398[1]
ZPE(H_2)	0.268	0.270	0.270[27]
ZPE(CH^+)	0.174	0.175	0.175[28]
Well depth (CH_2^+)	4.259	4.393	—

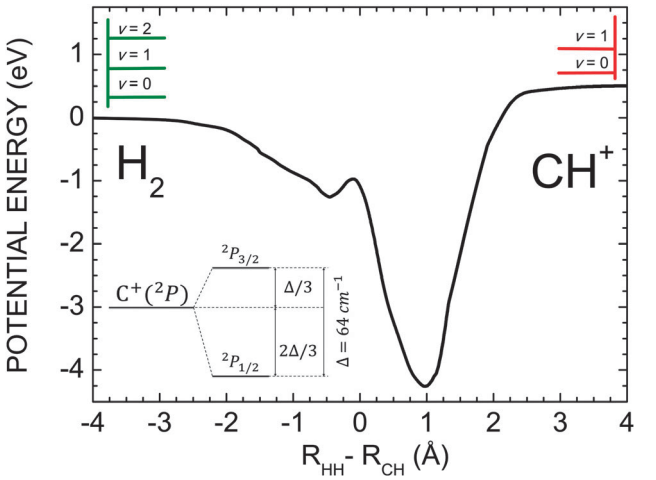

Fig. 1 Minimum energy path for the $C^+ + H_2 \rightarrow CH^+ + H$ reaction on the WS potential energy surface. The energy levels of the first vibrational states for both asymptotes are also included. The inset shows the spin–orbit splitting of the ^2P state of C^+.

Our analysis of the $C^+ + H_2$ reaction is based on QCT as well as on the statistical quasi-classical (SQCT) methodology.[25,26] The main characteristics of both procedures are summed up below.

2.1 Quasi-classical trajectory method

QCT calculations have been the basis of our analysis of the $C^+ + H_2$ reaction. To determine both the energy dependence of the integral cross section (excitation functions) and the rate coefficients, batches of 5×10^5 trajectories were integrated in the range of collision energies spanning from 10^{-4} to 1.5 eV by varying the collision energy continuously.[29] Since the maximum impact parameter at each collision energy, $b_{max}(E_{coll})$, changes (either decreasing or increasing) with E_{coll}, the impact parameter b for each trajectory was sampled by taking into account the dependence of b_{max} on E_{coll}. This dependence was previously determined with batches of trajectories run at discrete E_{coll}. Once the value of E_{coll} is randomly selected for each trajectory, the value

of b was sampled as $b = \xi^{1/2} b_{max}(E_{coll})$ where ξ is a random number in the [0,1] interval. Each trajectory is then weighted with $w_i = b_{max}^2(E_{coll})/D^2$, where D is the absolute maximum impact parameter in the whole calculation. The calculations covered the initial states $H_2(v = 0, j = 0–8)$ and $H_2(v = 1, j = 0–4)$, which are the reactant states considered in this study. Additional batches of 3×10^4 trajectories between 0.1 meV and 10 meV were analyzed in order to improve the accuracy of the calculations in this interval of collision energies. Finally, batches of 5×10^4 trajectories between 0.001 and 1.5 eV at $J = 0$ total angular momentum were integrated just for the initial states $H_2(v = 0–1, j = 0)$, following the methodology described in ref. 29.

In all cases, the integration step size was 0.05 fs, which guaranteed total energy (total angular momentum) conservation better than one part in $10^4(10^6)$. Due to the long range interaction in the entrance and exit channels, the trajectories were started and finished at an atom–diatom R distance of 20 Å. Special care was paid for an accurate (and computationally expensive) integration of trajectories at the lowest collision energies ensuring an acceptable total energy conservation.

The rovibrational energies of the diatomic molecules were determined by semiclassical quantization of the action using the asymptotes of the PES as potentials and their values were fitted to a Dunham expansion in $v + 1/2$ and $j(j + 1)$. The assignment of product quantum numbers at the end of each trajectory was performed by first equating the square of the classical CH^+ rotational angular momentum to $j'(j' + 1)\hbar$. The real value of j' obtained in this way is used to derive a real vibrational quantum number v' by equating the internal energy of the outgoing molecule to the Dunham expansion of the CH^+ rovibrational energies. In the simplest version of the assignment, the real numbers so obtained are rounded to the nearest integers. This is the so called histogram binning (HB) method. However, this procedure may not account properly for the zero point energy (ZPE) of the products, especially for endothermic reactions,[30,31] leading to the population of product states which are not energetically accessible. The Gaussian binning (GB) procedure provides an alternative wherein this problem can be at least partially overcome.[31–33] In this case, each trajectory is weighted according to a Gaussian function centered on the correct quantum mechanical vibrational actions: the closer the real vibrational quantum number of a given trajectory to the center of the Gaussian, the larger the weighting coefficient for that trajectory. Trajectories whose vibrational action is far from the quantum mechanical ones contribute very little to the cross section. The standard full-width half-maximum of 0.1 for the Gaussian functions was used in the present work.

2.2 QCT rate coefficients

The initial state-selected rate coefficients are obtained directly from the QCT data by means of the expression

$$k_{v,j}(T) = \int P_{MB}(E_{coll}|T)\sigma_{v,j}(E_{coll})v_r \mathrm{d}E_{coll} \approx \frac{\pi D^2}{N_{tot}}(E_2 - E_1)\sum_{i=1}^{N_r} w_i v_r^{(i)} P_{MB}\left(E_{coll}^{(i)}\middle|T\right) \quad (1)$$

where the second line is the Monte-Carlo evaluation of the integral. In this equation, $\sigma_{v,j}(E_{coll})$ is the integral cross section for the reaction in a selected (v,j) H_2 state, $(E_2 - E_1)$ is just the collision energy range considered in the sampling, $P_{MB}(E_{coll}^{(i)}|T)$ is the Maxwell–Boltzmann distribution, $v_r^{(i)}$ and $E_{coll}^{(i)}$ are the respective relative velocity and the translational (collision) energy corresponding to the i-th trajectory, N_{tot} is the total number of trajectories (reactive and inelastic) and D is the largest impact parameter in the whole set of trajectories. The sum runs over all the reactive trajectories starting in a (v,j) state. The weight for each trajectory, w_i, is given by the product of the weight assigned to the impact parameter in the sampling, $b_{max}^2(E_{coll})/D^2$, as indicated in Section 2.1,[29] times the weight assigned to the trajectory by the binning procedure used in the calculation (which in the case of the standard HB procedure would be either 0 or 1).[30,31,33]

In order to compare with the experimental rate coefficients it is necessary to consider the electronic partition function of the C^+ cation. Only the ground $^2P_{1/2}$ level correlates adiabatically with the product ground state *via* the $1^2A'$ PES. It is therefore necessary to take into account that only a fraction of the incident cations are in this spin–orbit level. Such a correction involves the electronic partition function referred to this state $Z_{el}^{[^2P_{1/2}]}(T)$:

$$Z_{el}^{[^2P_{1/2}]}(T) = 2 + 4\exp(-\beta\Delta_{so}) \quad (2)$$

The state specific rate coefficients corrected with the fraction of population in the $^2P_{1/2}$ state will be

$$k_{v,j}^{[^2P_{1/2}]}(T) = \frac{2}{2 + 4\exp(-\beta\Delta_{so})}k_{v,j}(T) \quad (3)$$

where $\beta = 1/k_B T$ and Δ_{so} = 7.9 meV (92.1 K or 64 cm^{-1}) is the spin–orbit splitting between the $^2P_{1/2}$ and $^2P_{3/2}$ states of the cation (see Fig. 1). The superscript $[^2P_{1/2}]$ indicates that the zero energy of the partition function is referred to the ground spin–orbit state.

The thermal rate coefficient averaged over the reactants' rovibrational states, $k(T)$, can be obtained from the state-selected rate coefficients by weighting them according to the Boltzmann distribution

$$k(T) = \sum_{v,j} w(v,j|T)k_{v,j}^{[^2P_{1/2}]}(T) \quad (4)$$

where $w(v,j|T)$ is precisely the Boltzmann weight of the initial v, j state at the temperature for which $k(T)$ is evaluated.

2.3 Statistical quasi-classical trajectory method

The SQCT method has been described in detail elsewhere.[25,26,34] It is equivalent to its quantal version (SQM)[35] with the sole difference that trajectories instead of wavefunctions are independently propagated in the exit and entrance channels. In spite of this difference, it has been demonstrated that the agreement between the SQM and SQCT approaches is almost perfect.[26,34]

The SQCT method uses a discrete sampling (quantization scheme) of the total and rotational angular momenta, as well as of the projection of the total angular momentum onto the body fixed axis. In contrast to the standard QCT method, trajectories are not integrated from the reactant to the product asymptotic regions but from both asymptotes until they are captured by the potential well. The corresponding capture points are characterized by a sufficiently negative value of the potential energy with respect to the asymptote where the integration begins. Such energies are chosen so as to assure that those trajectories that reach these values of energy have surmounted the centrifugal barrier and can be, in principle, considered as trapped in the potential well. Once integrated, the method proceeds by using the trajectories to calculate capture probabilities for all the possible arrangement channels and for all the energetically open reactant and product states at a given total energy. Given the capture probabilities, reaction probabilities and integral and differential cross section are in turn calculated using equations identical to those used in the SQM model,[25,26,35] the quantum mechanical version of the method.

Essential in the statistical model is the implicit assumption that the only requirement for the formation of the complex is the occurrence of the capture; that is, the overcoming of the centrifugal barrier (or its effective counterpart if there exists an additional dynamical barrier). Once the barrier is surmounted and the system reaches the "chemical" region which, for statistical reactions, corresponds to the well region, it is implicitly surmised that the complex has been formed. Furthermore, its lifetime is assumed to be long enough to ensure the randomization of the energy among the different modes, in such a way that the outcome is purely statistical. As we will see, this assumption is not necessarily correct, and in this case, surmounting the barrier does not imply the formation of a sufficiently long-lived complex.

For the present work, the SQCT method was applied by integrating trajectories for 25 collision energies compressed in the 1 meV to 1.0 eV interval. An integration time step of 0.01 fs was chosen so as to guarantee conservation of total energy better than one part in 10^5 and conservation of total angular momentum better than one part in 10^6. The number of trajectories integrated was 2×10^5 per channel and the capture potentials were selected as −1.0 eV and −0.4 eV, referred to the H_2 and CH^+ asymptotes respectively.

3 Results and discussion

3.1 Integral cross sections

Fig. 2 presents the $J = 0$ reaction probabilities as a function of the collision energy for the $C^+ + H_2(v = 0–1, j = 0–1) \rightarrow CH^+(v' = \text{all}, j' = \text{all}) + H$ reactions. The reaction probabilities for $v = 0$ (top panel) and $v = 1$ (bottom panel) are conspicuously different; while in the first case the reaction presents a threshold which roughly coincides with the reaction endothermicity, the reaction probability of vibrationally excited H_2 displays no threshold and decays rapidly at low collision energies. Such different behaviour can be easily explained in terms of the data shown in Table 1 and

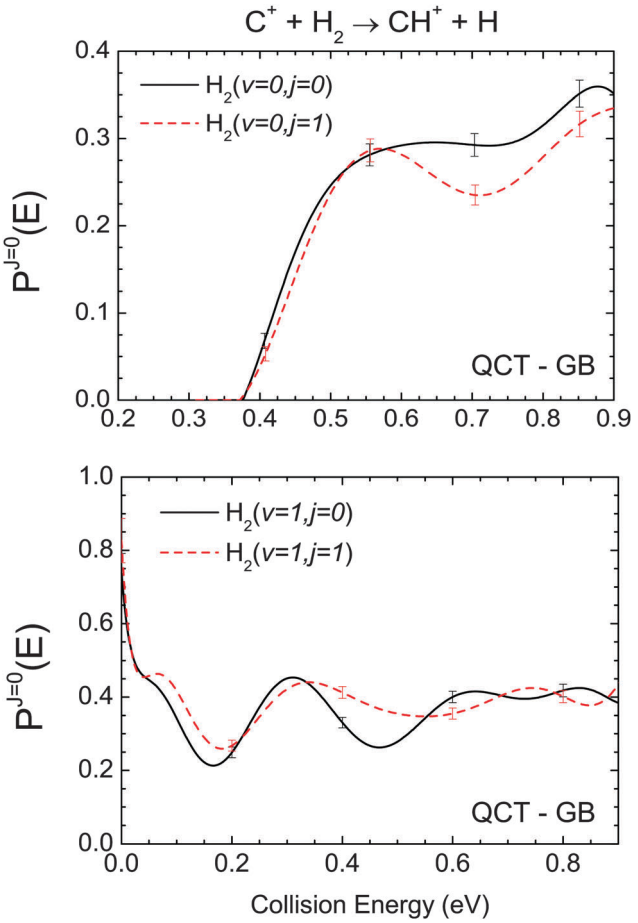

Fig. 2 QCT-GB zero total angular momentum ($J = 0$) reaction probabilities for the $C^+ + H_2(v = 0–1, j = 0–1) \rightarrow CH^+ + H$ reactions summed over all final state reactions as a function of the collision energy. The error bars indicate the statistical errors of the calculations (one standard deviation).

the minimum energy path presented in Fig. 1. Whereas the ground vibrational state of the reactants lies below the product asymptote, the addition of one H_2 vibrational quantum ($\approx$0.78 eV) is sufficient to reach the ground state product level and the reaction behaves as a barrierless one. In both cases, the reaction probability displays some broad oscillations around a constant value for energies well above the threshold ($v = 0$) or above zero ($v = 1$). In turn, rotational excitation of the reactants into $j = 1$ does not alter significantly either the shape or the values of the reaction probability. As it will be shown hereunder, however, higher rotational states have a very positive influence on the reactivity.

The TDWP QM $J = 0$ reaction probabilities (see ref. 19) calculated on the SH PES are similar in shape but slightly larger than the present QCT results on the WS PES, leaving aside the sharp and fast oscillations due to a congested resonance structure caused by the intermediate CH_2^+ deep well. Once the TDWP oscillations are averaged out, the small differences are likely due to the discrepancies in the energetics of the SH and WS PESs, as shown in Table 1. The agreement is better for the $v = 1$ reaction probability, where those discrepancies are much less relevant due to the inherent exoergicity of the process.

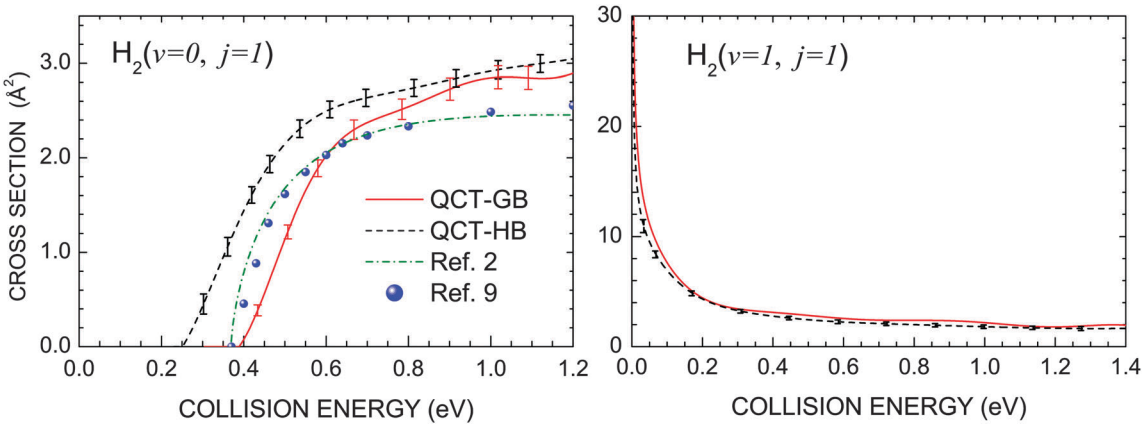

Fig. 3 Total integral cross section for the $C^+ + H_2(v = 0–1, j = 1) \rightarrow CH^+(v' = \text{all}, j' = \text{all}) + H$ reactions as a function of the collision energy. Theoretical results, including the statistical error bars, correspond to QCT-GB and QCT-HB calculations. For the sake of comparison, available experimental data[2,9] are presented in the left panel.

The excitation functions for the $C^+ + H_2(v = 0–1, j = 1)$ reactions are presented in Fig. 3. As expected, for $v = 0$ collisions, the agreement between the two theoretical methods is extremely poor near the threshold, whose value is largely underestimated by the HB calculations, although it improves as the collision energy increases. The deconvoluted experimental data,[9] extracted from a gas-guide ion beam arrangement corresponding to collisions at a rotational temperature of 380 K, where $j = 1$ is the most populated rotational state, have been scaled to the QCT-GB results with a factor of 1.25 so as to make the comparison easier. Similarly, the excitation function derived by Ervin and Armentrout[2] from their guide ion beam experiments has also been scaled to the present theoretical GB-excitation function (and in turn, to that from ref. 9) using a factor of 1.38. It should be pointed out that these deconvoluted excitation functions are tentative models (not unique) that once averaged over the spread of the collision energy render, with approximate accuracy, the actual experimental measurements. Apart from the overall scaling factor, the present QCT-GB calculations lead to smaller values in the post-threshold region but clearly higher at energies above 0.7 eV. However, it should be taken into account that the $^2P_{1/2}$ relative population has not been included in the value of the cross sections. Assuming a purely thermal population of the atomic states, the QCT-GB results would need to be multiplied by a factor of ≈ 0.4 and hence the cross sections would be considerably smaller than those derived from the experiment. This discrepancy is not surprising considering that the WS PES overestimates the endoergicity by 22 meV. The effect of this seemingly small difference will be discussed below.

Regarding the $C^+ + H_2(v = 1, j = 1)$ collisions (right panel), conservation of the product zero point energy is not as critical as for $v = 0$ reactants and the corresponding GB and HB excitation functions are in close agreement over the whole range of energies. In both HB and GB cases, the excitation functions display the normal profile for a barrierless reaction; *i.e.*, they show a continuous decrease as the collision energy gets larger.

The present theoretical results can be compared with the TDWP results by Zanchet *et al.*[19] carried out on the SH PES. For that PES, the endothermicity is, in contrast, underestimated (see Table 1) and hence the resulting cross sections and rate coefficients can be expected to be larger than those calculated in this work.

The breakdown of the excitation functions into its different vibrational contributions for the $C^+ + H_2(v = 0–1, j = 0–1)$ reactions is presented in Fig. 4. For the upper panels ($v = 0$), the v'-resolved excitation functions evolve differently once both channels get opened; while the curve for $v' = 0$ decreases monotonically, the contrary applies to its $v' = 1$ counterpart. As expected, when one vibrational quanta is added to the reactants (bottom panels) only those collisions leading to $CH^+(v' = 0)$ formation exhibit no threshold. In any other case ($v' = 1$ and 2), the collisions show an increasingly larger threshold. It is interesting to highlight that, for large enough energies, the excitation functions for $v' = 0$, 1 and 2 converge around a value approximately one third of the total one. Such behaviour suggests that the internal energy is distributed almost evenly among all the open internal states. As it will be discussed below, $v = 0$ collisions with different degrees of rotational excitation give rise to vibrationally resolved excitation functions whose values tend to converge at sufficiently high E_{coll}.

In view of the previous discussion, one could wonder if the deep well present in the surface renders the reaction statistical. In order to get an answer to this question, Fig. 5 compares SQCT and GB-QCT results for the $C^+ + H_2(v = 0–1, j = 0–1)$ reactions. As commented on above, the statistical model assumes that the collision complex is formed once the entrance barriers of both channels are surmounted. The significant disagreement exhibited by both types of calculations, where the SQCT method leads to much bigger cross sections, clearly indicates that this assumption is not correct and that the reaction dynamics cannot be described according to a purely, unbiased statistical model.

The influence of the rotation on the cross sections is illustrated in Fig. 6, where the total and v'-resolved excitation

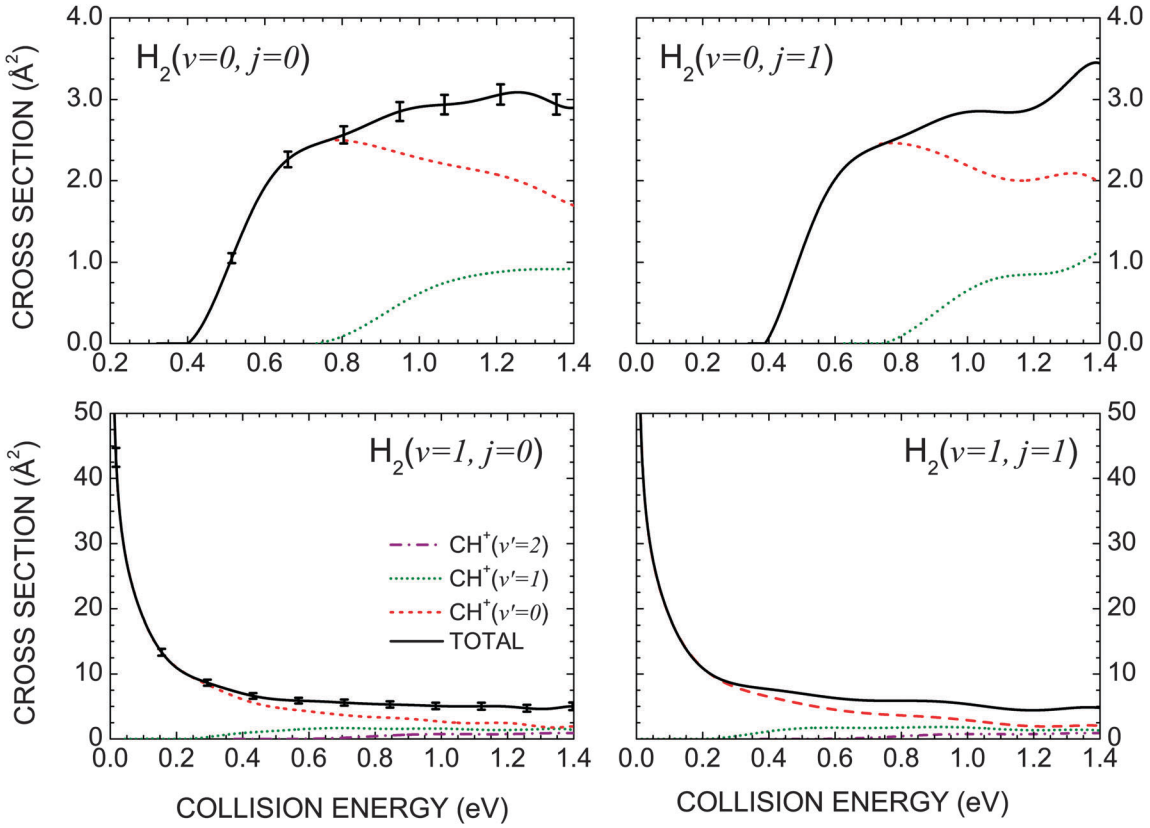

Fig. 4 Total (continuous black lines) and v' resolved (discontinuous red, green and purple lines) integral cross section as a function of the collision energy for the $C^+ + H_2(v = 0–1, j = 0–1)$ reactions. All results correspond to QCT-GB calculations. Statistical error bars, only included in the total results of the left panels, are of the same order of magnitude for all curves.

functions for the $C^+ + H_2(v = 0, j = 0, 4, 7$ and $8)$ reactions are presented. With increasing rotational excitation, up to $j = 7$, the threshold energy shifts towards lower values and the reactivity grows gradually. For $H_2(v = 0, j = 8)$, however, the internal energy of the reactants gets over the products ZPE and, in consequence, the collisions leading to $CH^+(v' = 0)$ formation display no threshold, and the excitation function follows the same pattern as with that observed with H_2 in $v = 1$. It can be concluded that the effect of rotational (and to a large extent of vibrational) excitation is mainly energetic and causes no significant change in the evolution of the v'-resolved excitation functions.

The evolution of the integral cross section at low collision energies for various initial states where the reaction threshold vanishes is illustrated in Fig. 7 as a log–log plot. As can be seen, the magnitude of the respective cross sections simply grows with the excess of internal energy above the endoergicity. Below 10^{-1} eV, the different curves become parallel straight lines characterized by a slope value equal to $-1/2$. This implies an energy dependence that conforms to the Langevin model. The relevance of this finding for the calculation of rate coefficients at very low temperatures which are of interest in astrophysical studies is enormous, as it makes possible to extrapolate accurately the values of the integral cross sections necessary for such calculations (see next section). Please notice that the cross section values presented in Fig. 7 have been calculated over the whole range of energies and not extrapolated.

3.2 Rate coefficients

Rate coefficients are more relevant in astrochemistry than integral cross sections when it comes to explaining the unexpectedly high abundance of CH^+ in the interstellar media. Values of the rate coefficients for the $C^+(^2P_{1/2}) + H_2(v = 0,1, j)$ collisions as a function of the temperature and for different rotational levels are given in Tables 2 and 3 for the reaction with H_2 in $v = 0$ and $v = 1$, respectively. The most remarkable result is that the values of the rate coefficients with high rotational excitations ($j \geq 7$) are comparable to those obtained with vibrational excitation.

This is further illustrated by Fig. 8, where total and v'-resolved $k_{v,j}^{[^2P_{1/2}]}(T; v')$ for the $C^+(^2P_{1/2}) + H_2(v = 0, j)$ reactions with increasing rotational excitation are presented as a function of the temperature. It must be pointed out that the represented rate coefficients include the electronic partition function, eqn (3). For low j values, the existence of an energetic threshold in the corresponding excitation function (see Fig. 6) leads to extremely small values of the rate coefficients at low temperatures. However, when $j = 7$, the threshold of the excitation function is almost null and, for $j = 8$, disappears. As a consequence, the increase in the rotational level of the

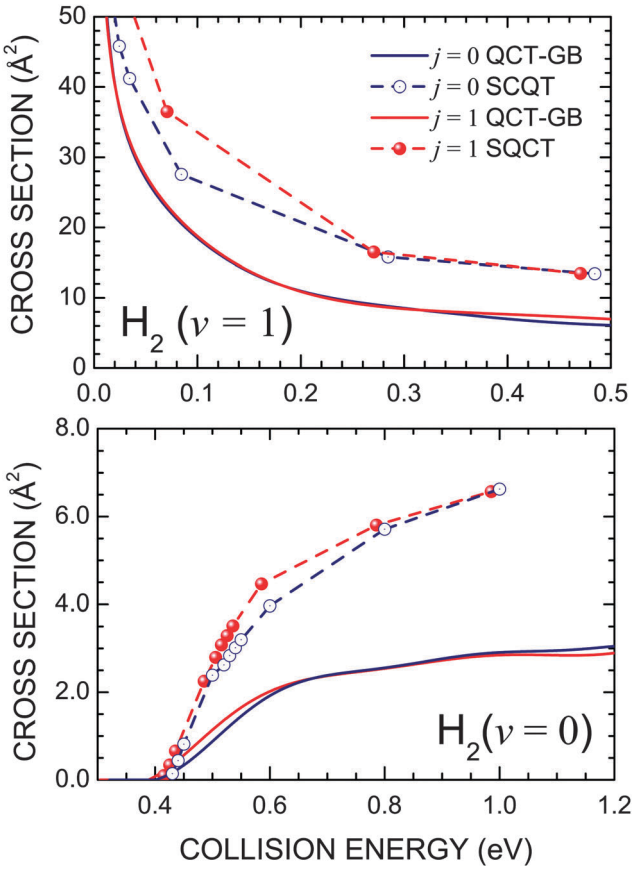

Fig. 5 Total integral cross section as a function of the collision energy for the $C^+ + H_2(v = 0–1, j = 0–1)$ reactions evaluated from QCT-GB (continuous lines) and SQCT (dashed lines) calculations.

reactants leads to a significant increase of the rate coefficients over the whole range of temperatures, and for $j \geq 8$ the rate coefficient behaviour is that of a reaction with no activation energy. For comparison purposes, similar plots of the rate coefficients for the $C^+ + H_2(v = 1, j = 0–4)$ reactions are represented in Fig. 9. As can be seen, in all cases the behaviour is essentially the same irrespective of the rotational quantum number and moreover similar to that found for $k_{v,j}^{[^2P_{1/2}]}(T)$ corresponding to $j = 8$ or higher.

Previous studies[9,10] have shown that vibrational excitation of the H_2 molecule increases the values of the rate coefficients at low temperatures very significantly, and it was expected that this effect could explain the observed abundance of the CH^+ molecule. To date, the most reliable theoretical determination of rate coefficients for the reaction with vibrationally excited H_2 has been that of Zanchet *et al.*[19] which were found to be considerably lower than those estimated by Hierl *et al.*[10] However, adopting these new data in the chemical models of the diffuse inter-stellar medium the observations of CH^+ could not be explained.

The present results indicate that vibrational excitation is not the only possible mechanism to explain the huge increase of the rate of CH^+ formation and that, in fact, rotational excitation makes possible to achieve a similar effect. The key point is, in both cases, to have enough internal energy as to overcome the endothermicity because, under these conditions, the rate coefficients at low temperature become significantly large due to the absence of threshold in the reaction.

An interesting finding is that the values of the rate coefficients at sufficiently low temperatures are well accounted for by the energy dependence of the Langevin model for collisions where the internal (either vibrational or rotational) excitation is sufficient to overcome the reaction endothermicity. The validity of such a model, which predicts a rate coefficient independent of temperature, is supported by the state-selected excitation functions in Fig. 7 at low collision energies (see discussion above).

The rate coefficients obtained using the Langevin model, *i.e.*, extrapolating the integral cross sections at low temperatures using the $\sigma_R(E_{col}) = AE_{col}^{-1/2}$ function and fitting the A coefficient using the data from Fig. 7 at $E_{coll} \leq 0.1$ eV are depicted in Fig. 10. It must be stressed that the represented rate coefficients are calculated using eqn (3) which contains the thermal population of the lowest $^2P_{1/2}$ state of the carbon cation. Accordingly, at very low T, the rate coefficients are temperature independent, as they correspond to the Langevin model. As the T rises, the population of the lowest $^2P_{1/2}$ state diminishes towards its limit of 1/3 at a sufficiently high temperature, and this factor makes $k(T)$ to decrease at higher T. In addition, from Fig. 7 it seems that the excitation function decreases more rapidly than $E_{coll}^{-1/2}$ at energies above 0.1 eV thus favouring a further decrease in the rate coefficient.

Finally, in order to compare the present calculations with the available experimental results,[10] thermal rates have been computed according to eqn (4). The comparison is shown in Table 4 and plotted in Fig. 11, where the solid black line represents the thermal rate coefficients for the title reaction, obtained from eqn (4). As observed, the QCT $k(T)$ underestimates the high temperature flowing afterglow thermal rate coefficients (mainly due to the reaction with H_2 in $v = 0$) determined by Hierl *et al.*[10] in the measured range of temperatures. However an important consideration is in order. As already mentioned, the theoretical endothermicity predicted by the WS PES is 22 meV (=255.3 K) larger than the experimental value (see Table 1). Since the reaction threshold is mainly governed by the value of ΔH_0°, it is not surprising that the predicted rate coefficients are systematically lower than the experimental ones. Moreover, as has been shown in this and previous sections, the enhancement of the reactivity with the reactant's internal energy is largely independent of whether it is deposited as vibrational or rotational energy. This finding also seems to indicate that the overall reactivity is likely to be largely insensitive to the particular features of the PES and, in particular, to the submerged barrier within the well shown in Fig. 1.

We therefore suggest an approximate correction to the rate coefficients that could be written as

$$k^{corr}(T) = e^{255.3/T} \sum_{v,j} w(v,j|T) k_{v,j}^{[^2P_{1/2}]}(T) \qquad (5)$$

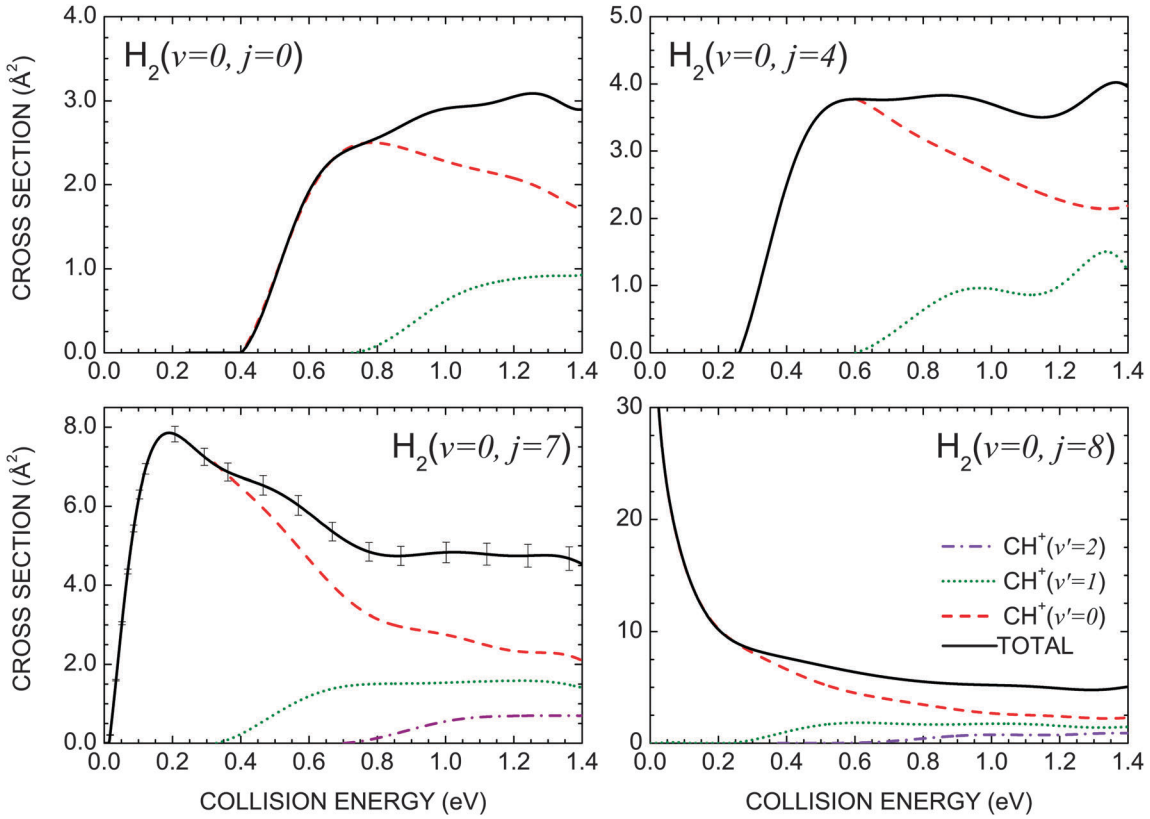

Fig. 6 Total (continuous black lines) and v' resolved (discontinuous red, green and purple lines) integral cross sections as a function of the collision energy for the $C^+ + H_2(v = 0, j = 0, 4, 7$ and 8) reactions. All results correspond to QCT-GB calculations. Statistical error bars, only included in the total results of the bottom-left panel, are of the same order of magnitude for all curves.

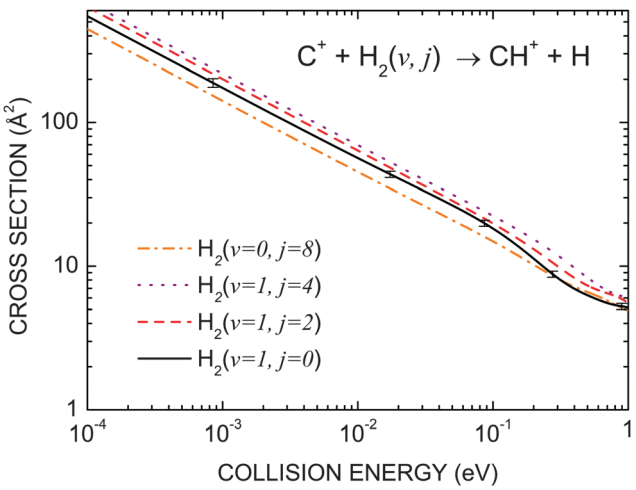

Fig. 7 Logarithmic representation of state-selected integral cross sections for different initial states of the $C^+ + H_2$ reaction. All results correspond to QCT-GB calculations. Statistical error bars, only included for the $C^+ + H_2(v = 1, j = 0)$ reaction, are of the same order of magnitude in all cases.

Table 2 State selected rate coefficients, $k_{v,j}^{[^2P_{1/2}]}(T)$, in $cm^3\ s^{-1}$, based on QCT-GB calculations for the $C^+ + H_2(v = 0, j)$ reaction as a function of the temperature. The values of the rate coefficients have been multiplied by the relative population of the ground electronic state $^2P_{1/2}$ (see eqn (2) and (3) of Section 2.2). The numbers within parentheses indicate the powers of 10. The omitted values are $<10^{-30}$ $cm^3\ s^{-1}$

T/K	$j = 0$	$j = 1$	$j = 3$	$j = 5$	$j = 7$	$j = 8$
50	—	—	—	—	1.2 (−12)	3.0 (−10)
100	—	—	1.6 (−27)	2.8 (−21)	3.4 (−12)	2.5 (−10)
200	1.1 (−21)	2.3 (−21)	2.0 (−19)	2.8 (−16)	1.1 (−11)	2.2 (−10)
300	3.5 (−18)	6.7 (−18)	1.4 (−16)	1.8 (−14)	2.1 (−11)	2.1 (−10)
500	2.9 (−15)	4.2 (−15)	3.2 (−14)	5.9 (−13)	4.0 (−11)	2.0 (−10)
800	1.4 (−13)	1.8 (−13)	3.6 (−13)	7.1 (−13)	6.4 (−11)	1.9 (−10)
1000	5.4 (−13)	6.5 (−13)	2.0 (−12)	8.8 (−12)	7.5 (−11)	1.9 (−10)
1500	3.3 (−12)	3.7 (−12)	8.4 (−12)	2.2 (−11)	9.6 (−11)	1.8 (−10)
2000	8.2 (−12)	8.8 (−12)	1.7 (−11)	3.6 (−11)	1.1 (−10)	1.7 (−10)
2500	1.4 (−11)	1.5 (−11)	2.6 (−11)	4.8 (−11)	1.2 (−10)	1.7 (−10)
3000	2.0 (−11)	2.1 (−11)	3.4 (−11)	5.7 (−11)	1.2 (−10)	1.7 (−10)
3500	2.5 (−11)	2.7 (−11)	4.6 (−11)	6.5 (−11)	1.3 (−10)	1.7 (−10)
4000	3.0 (−11)	3.1 (−11)	5.1 (−11)	7.1 (−11)	1.3 (−10)	1.7 (−10)

Note that this correction is mathematically equivalent to reduce the barrier to the reaction by just the difference of the reaction endothermicity. The thermal rate coefficients modified by the factor of eqn (5) are also shown in Fig. 11 (green dashed line). Both results are compared with experimental data from Hierl *et al.*[10] so that, as it can be observed, the corrected QCT thermal rates match closely the experimental results.

In ref. 10, the authors also reported the so called "rate coefficient at temperature T for a given vibrational state". Specifically, they estimated the $v = 1$ thermal rate coefficients at temperatures above 800 K by subtracting from the thermal rate coefficients (shown in Fig. 11 as black dots) approximate

Table 3 State selected rate coefficients $k_{v,j}^{[^2P_{1/2}]}(T)$, in $cm^3\ s^{-1}$, based on QCT-GB calculations for the $C^+ + H_2(v = 1, j)$ reactions as a function of the temperature. The values of the rate coefficients have been multiplied by the relative population of the ground electronic $^2P_{1/2}$ state (see eqn (2) and (3) of Section 2.2). The numbers within parentheses indicate the powers of 10

T/K	$j = 0$	$j = 1$	$j = 2$	$j = 3$	$j = 4$
50	4.0 (−10)	4.0 (−10)	4.3 (−10)	4.5 (−10)	4.4 (−10)
100	3.1 (−10)	3.1 (−10)	3.4 (−10)	3.5 (−10)	3.5 (−10)
200	2.7 (−10)	2.7 (−10)	2.9 (−10)	3.0 (−10)	3.1 (−10)
300	2.4 (−10)	2.5 (−10)	2.7 (−10)	2.8 (−10)	2.8 (−10)
500	2.3 (−10)	2.4 (−10)	2.6 (−10)	2.7 (−10)	2.7 (−10)
800	2.1 (−10)	2.2 (−10)	2.4 (−10)	2.5 (−10)	2.6 (−10)
1000	2.1 (−10)	2.1 (−10)	2.3 (−10)	2.4 (−10)	2.6 (−10)
1500	1.9 (−10)	2.0 (−10)	2.2 (−10)	2.3 (−10)	2.5 (−10)
2000	1.9 (−10)	1.9 (−10)	2.1 (−10)	2.2 (−10)	2.4 (−10)
2500	1.8 (−10)	1.9 (−10)	2.1 (−10)	2.2 (−10)	2.3 (−10)
3000	1.8 (−10)	1.8 (−10)	2.0 (−10)	2.1 (−10)	2.3 (−10)
3500	1.7 (−10)	1.8 (−10)	2.0 (−10)	2.1 (−10)	2.2 (−10)
4000	1.7 (−10)	1.8 (−10)	1.9 (−10)	2.0 (−10)	2.2 (−10)

rate coefficients for $v = 0$. These $k(T,v = 0)$ were calculated using the guided ion beam data obtained by Erwin and Armentrout[2] at various collision energies, which were equated to $3/2k_BT$. The experimental data from ref. 2, however, were obtained at a target temperature of ≈300 K, and hence at a fixed H_2 vibrational and rotational temperature of 300 K. The resulting $v = 1$ rate coefficients are shown in Fig. 11 as (black) open circles with values about 2.0×10^{-9} $cm^3\ s^{-1}$, which are of the order of magnitude of the rate coefficients that could be derived from the Langevin model.

In order to compare with these estimates, the thermal data for $v = 1$ were calculated using the $k_{v=1,j}^{[^2P_{1/2}]}(T)$ data shown in Table 3 and Fig. 9 by averaging over the rotational distributions for this vibrational state according to

$$k(T; v = 1) = \sum_j \frac{w(v = 1, j|T)}{w(v = 1|T)} k_{v=1,j}^{[^2P_{1/2}]}(T), \qquad (6)$$

where $w(v = 1|T)$ is the sum of the weights $w(v = 1,j|T)$ of all the rotational states of the $v = 1$ manifold. A similar equation was used for the "corrected" rate coefficients including the exponential factor intended to compensate the larger endothermicity of the PES with respect to the experimental one. As shown in Fig. 11, the present calculations (dashed and short-dashed lines) predict rate coefficients which are nearly ten times smaller than those derived by Hierl *et al.*[10] In particular, at a temperature of 800 K the value provided in ref. 10 is 2.5×10^{-9} $cm^3\ s^{-1}$, while our prediction is 2.4×10^{-10} $cm^3\ s^{-1}$ for the $v = 1$ thermal rate coefficient. With the correction performed in eqn (5), the resulting value is 3.1×10^{-10} $cm^3\ s^{-1}$, still a factor of 8 lower than that reported in ref. 10. In ref. 19, Zanchet *et al.* calculated the QM thermal rate

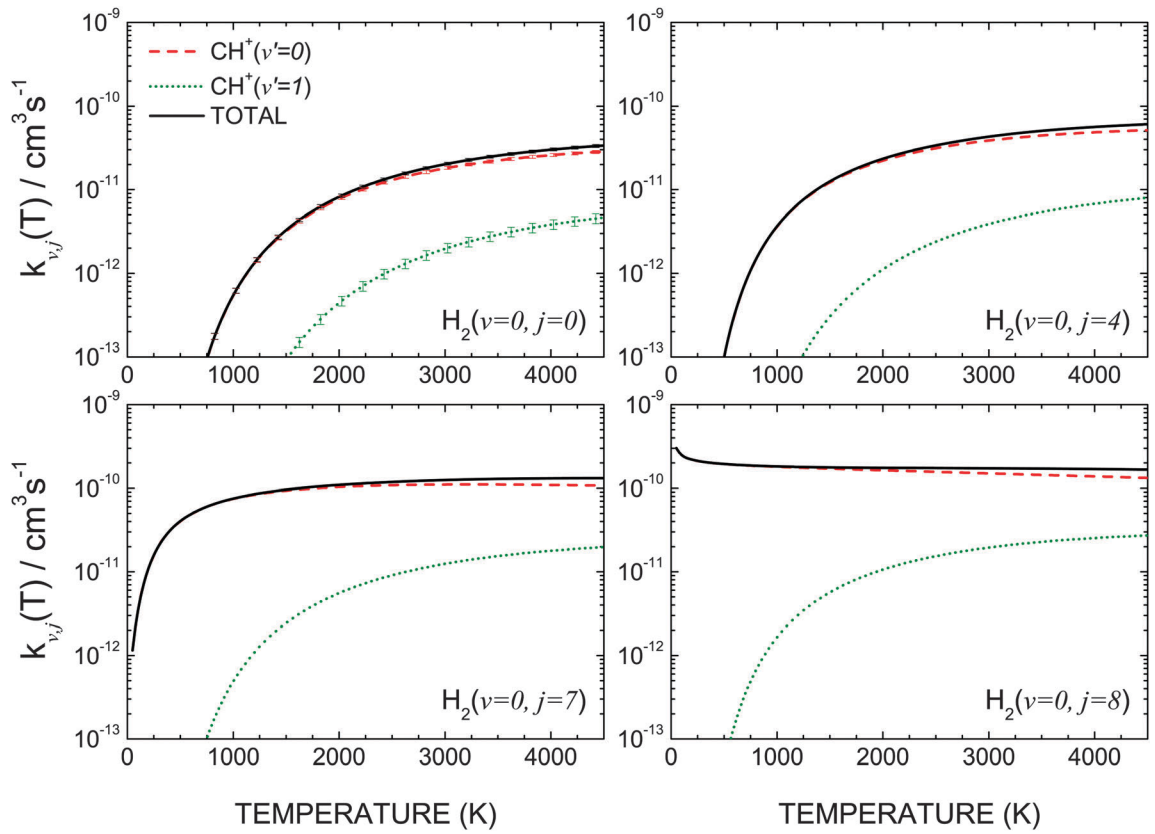

Fig. 8 Total (continuous black lines) and v' resolved (discontinuous red and green lines) rate coefficients as a function of the temperature for the $C^+ + H_2(v = 0, j = 0, 4, 7$ and 8) reactions. All results derive from QCT-GB calculations and correspond to temperatures above 50 K. Statistical error bars, only included in the top-left panel, are of the same order of magnitude for all curves. The electronic partition function is included in the calculations according to eqn (3).

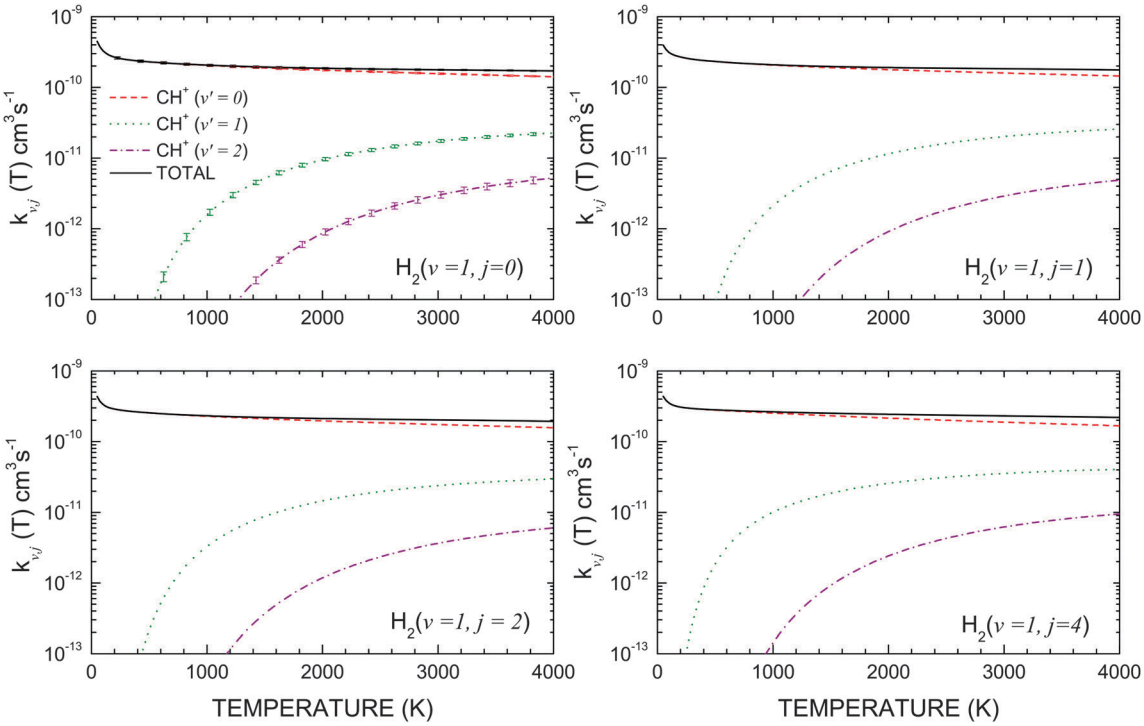

Fig. 9 As Fig. 8 but for the $C^+ + H_2(v = 1, j = 0, 1, 2, 4)$ reactions.

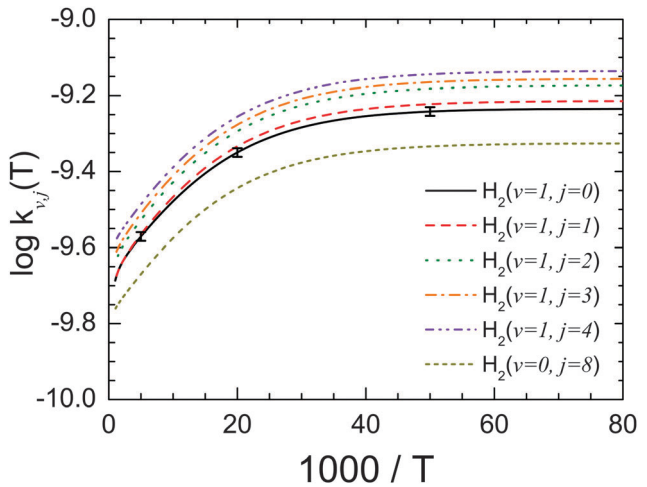

Fig. 10 Arrhenius plot of the total rate coefficients as a function of the inverse of temperature for the $C^+ + H_2(v = 0, j = 8)$ and $C^+ + H_2(v = 1, j = 0–4)$ reactions. The values of the rate coefficients have been calculated from integral cross sections extrapolated following the energy dependence of the Langevin model. The statistical error bars are shown for the reaction with $H_2(v = 1, j = 0)$. All results correspond to QCT-GB calculations.

Table 4 Comparison of QCT-GB based thermal (averaged over all rovibrational states) rate coefficients, eqn (4) and thermal "corrected" eqn (5), with the high temperature flowing afterglow experimental rate coefficients[10] in $cm^3\ s^{-1}$ for the $C^+(^2P_{1/2}) + H_2$ reaction as a function of the temperature

T/K	QCT thermal	Thermal corrected	Exp.
400	7.3 (−15)	1.4 (−14)	5.5 (−15)
500	6.3 (−14)	1.1 (−13)	9.2 (−14)
600	2.7 (−13)	4.2 (−13)	4.8 (−13)
700	7.9 (−13)	1.1 (−12)	1.2 (−12)
800	1.7 (−12)	2.4 (−12)	2.5 (−12)
900	3.2 (−12)	4.2 (−12)	5.1 (−12)
1000	5.2 (−12)	6.7 (−12)	8.3 (−12)
1100	7.6 (−12)	9.6 (−12)	1.2 (−11)
1200	1.1 (−11)	1.3 (−11)	1.7 (−11)
1300	1.4 (−11)	1.7 (−11)	2.1 (−11)
1400	1.7 (−11)	2.0 (−11)	—

coefficients for $v = 1$ and $j = 0$, 1 giving rise to a value of $3.0 \times 10^{-10}\ cm^3\ s^{-1}$. These calculations were performed on the SH PES,[17] whose endothermicity is 28 meV (324 K) smaller than the experimental value. If the same correction as that used in eqn (5) is applied to this value, the result would be $2.1 \times 10^{-10}\ cm^3\ s^{-1}$, where now the exponential factor contains a negative value of −28 meV corresponding to the lower endothermicity with respect to the experimental data. Therefore, present and previous calculations carried out on different PESs and with different methodologies render values of about a factor of 10 lower than the estimate reported in ref. 10.

Apart from the inherent approximations included in the derivation of the rate coefficients for $v = 1$, the method used by Hierl *et al.* is flawed by the assumption that rotation in $v = 0$ does not enhance the reactivity, and that a 300 K H_2 rotational temperature could account for the $k(T|v = 0)$ data. In the present work we have shown that for $j > 7$ the influence of rotation is comparable to that of vibration. To further show that this is the case, we have simulated the derivation by Hierl *et al.* using the present theoretical results using the following formula

$$k^{\mathrm{simul}}(T, v = 1) = \frac{k(T) - k^{[^2P_{1/2}]}_{v=0,j=1}(T)w(v = 0|T)}{w(v = 1|T)} \qquad (7)$$

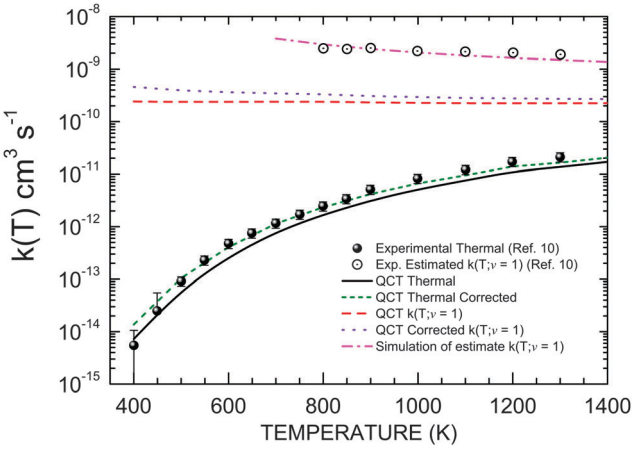

Fig. 11 Comparison of the experimental (black filled circles) thermal rate coefficients from ref. 10 for the $C^+ + H_2$ reaction with the corresponding QCT results (black solid line) averaged over the Boltzmann distribution of internal states according to eqn (4). The corrected $k^{corr}(T)$, evaluated with eqn (5), (green dashed lines) are also shown. The thermal and corrected thermal rate coefficients for the $C^+ + H_2(v = 1)$ reaction calculated according to eqn (6) are shown as red dashed line and violet short-dashed line, respectively. The results are compared to the experimentally derived $k(T;v = 1)$ (open black points) from ref. 10, and with the "simulated" $k^{simul}(T,v = 1)$ (pink dot-dash line) according to eqn (7) (see the text for more details).

where $w(v = 0|T)$ and $w(v = 1|T)$ are the respective thermal populations of $v = 0$ and $v = 1$ calculated by summing over the weights of all rotational states of each vibrational manifold. This formula is equivalent to substitute each of the j-selected $k^{[^2P_{1/2}]}_{v=0,j}(T)$ rate coefficients by $k^{[^2P_{1/2}]}_{v=0,j=1}(T)$. The $k^{simul}(T,v = 1)$ results are represented in Fig. 11 by a (pink) dash-dotted line that, as expected, mimic almost perfectly the estimate of $k(v = 1|T)$ by Hierl.

At $T = 800$ K, the $v = 0$ and $v = 1$ contributions to the total thermal $k(T)$ are 1.6×10^{-12} cm^3 s^{-1} and 1.3×10^{-13} cm^3 s^{-1} when the actual rotationally dependent rate coefficients are used. If instead eqn (7) is used, the contribution from $v = 0$ would just be 1.8×10^{-13} cm^3 s^{-1} hence comparable to that of $v = 1$. The importance of high rotational states cannot be neglected; at $T = 800$ K the population in $j = 8$ is 20 times larger than that of $v = 1, j = 0$ and almost three times than that of $v = 1$ and $j = 1$ (in spite of the favourable weight of the *ortho*-H_2 species).

The values and temperature dependence of the derived $k(v = 1,T)$ by Hierl *et al.* have been long used in the astrophysical models to explain the abundance of the CH^+ species. The present results confirm those calculated by Zanchet *et al.*[19] and strongly suggest that values of $\approx 2 \times 10^{-9}$ cm^3 s^{-1}, close to what a simple Langevin model would predict, constitute an overestimation of the $v = 1$ rate coefficient which is likely to be one order of magnitude smaller. Moreover, the present work indicates that a reliable simulation must take into account the effect of the rotational excitation incorporating $v = 0$ rotational states whose population can exceed that of the $v = 1$ manifold.

4 Conclusions

We have performed a dynamical study of the $C^+ + H_2(^1\Sigma_g^+) \rightarrow CH^+ + H$ reaction using quasiclassical trajectory (QCT) calculations on the PES produced by Warmbier and Schneider. State-selected integral cross sections and rate coefficients have been calculated using QCT for $v = 0, j = 0$–8, and $v = 1, j = 0$–4 initial states. To overcome the problem associated with the non-conservation of the zero point energy of the products, especially acute in the case of endothermic reactions, the Gaussian binning procedure has been used.

The main issue of this work has been the analysis of the H_2 internal energy on the reactivity of this system characterized by an endothermic barrierless potential energy surface. In particular, we have focused on the comparative effects of the vibrational and rotational excitation of the H_2 molecule. It has been found that any internal excitation of the reactants has a similar effect: it necessarily causes the threshold to decrease and, finally, when the internal energy is greater than the endothermicity, to disappear. This threshold cancellation is accompanied by an abrupt change of the behaviour displayed by the reactive cross sections, which adopt the typical profile for barrierless reactions. The present study corroborates that rotational excitation is as effective as vibration to promote the reactivity and it could therefore be another possible explanation for the abundance of CH^+ in the interstellar media.

The present analysis has also shown that, for those initial states where no threshold exists, the cross sections at collision energies below 0.1 eV display a $\propto E^{1/2}$ dependence which facilitates the extrapolation at even lower collision energies for which the QCT (or any other time dependent calculation) is not practical. Consequently, the rate coefficients at low temperatures derived from the calculations follow a nearly temperature independent behaviour. In spite of this, it is important to stress that the absolute values of the rate coefficients predicted by the Langevin model (typically 1–3 $\times 10^{-9}$ cm^3 s^{-1}) are one order of magnitude above those found in the present and in some other previous calculations.

It has been also shown that, in spite of the deep well present in the potential energy surface, the behaviour of the reaction is not statistical as evinced by calculations using rigorous statistical models whose results deviate from those found in the QCT calculations.

The importance of the rotational excitation has also been exemplified by the discussion of the accordance between experimentally derived and theoretical results for the $v = 1$ rate coefficients. Present and previous theoretical studies reported by Zanchet *et al.*[19] render values one order of magnitude smaller than those experimentally estimated. The present work shows that this disagreement stems from disregarding the effect of the rotational excitation on the $v = 0$ rate coefficients in the experimental derivation.

Although the accuracy of the present results is partly limited by the accuracy of the PES, which predicts an endothermicity larger than the experimental one, and perhaps by the possible limitations of the QCT methodology, the present study serves to

demonstrate the importance of rotational excitation and to corroborate that the rate coefficients for the reaction with H_2 in $v = 1$ are well below the until recently assumed Langevin behaviour. Future astrophysical models should incorporate the dependence of the H_2 rotational excitation on the reactivity.

Acknowledgements

The authors are grateful to Dr Octavio Roncero for useful discussions and for letting us know the results of ref. 19 in advance. The funding by the Ministries of Science and Innovation and Economy and Competitiveness (grants CTQ2008-02578, CTQ2012-37404-C02, and Consolider Ingenio 2010 CSD2009-00038) is acknowledged. DH also acknowledges the FPU fellowship AP2009-0038.

References

1 K. Ervin and P. Armentrout, *J. Chem. Phys.*, 1984, **80**, 2978.
2 K. M. Ervin and P. B. Armentrout, *J. Chem. Phys.*, 1986, **84**, 6738.
3 K. M. Ervin and P. B. Armentrout, *J. Chem. Phys.*, 1986, **84**, 6750.
4 A. E. Douglas and G. Herzberg, *Astrophys. J.*, 1941, **94**, 381.
5 W. B. Maier II, *J. Chem. Phys.*, 1967, **46**, 4991.
6 E. Lindemann, L. C. Frees, R. W. Rozett and W. S. Koski, *J. Chem. Phys.*, 1972, **56**, 1003.
7 C. R. Iden, R. Liardon and W. S. Koski, *J. Chem. Phys.*, 1972, **56**, 851.
8 B. H. Mahan and T. M. Sloane, *J. Chem. Phys.*, 1973, **59**, 5661.
9 D. Gerlich, R. Disch and S. Scherbarth, *J. Chem. Phys.*, 1987, **87**, 350–359.
10 P. M. Hierl, R. A. Morris and A. A. Viggiano, *J. Chem. Phys.*, 1997, **106**, 10145.
11 D. G. Truhlar, *J. Chem. Phys.*, 1969, **51**(10), 4617.
12 E. Herbst, *Chem. Phys. Lett.*, 1977, **47**, 517.
13 J. Sullivan and E. Herbst, *Chem. Phys. Lett.*, 1978, **55**, 226.
14 C. Galloy and J. Lorquet, *Chem. Phys.*, 1978, **30**, 169.
15 R. Jaquet and V. Staemmler, *Chem. Phys.*, 1982, **68**, 479.
16 S. Sakai, S. Kato, K. Morokuma and I. Kusunoki, *J. Chem. Phys.*, 1981, **75**, 5398.
17 T. Stoecklin and P. Halvick, *Phys. Chem. Chem. Phys.*, 2005, **7**, 2446–2452.
18 P. Halvick, T. Stoecklin, P. Larregaray and L. Bonnet, *Phys. Chem. Chem. Phys.*, 2007, **9**, 582.
19 A. Zanchet, B. Godard, N. Bulut, O. Roncero, P. Halvick and J. Cernicharo, *Astrophys. J.*, 2013, **766**, 80.
20 R. Warmbier and R. Schneider, *Phys. Chem. Chem. Phys.*, 2011, **13**, 10285–10294.
21 A. E. Douglas and G. Herzberg, *Astrophys. J.*, 1941, **94**, 381.
22 B. Godard, E. Falgarone, M. Gerin, D. C. Lis, M. D. Luca, J. H. Black, J. R. Goicoechea, J. Cernicharo, D. A. Neufeld, K. M. Menten and M. Emprechtinger, *Astron. Astrophys.*, 2012, **540**, A87.
23 M. Agúndez, J. R. Goicoechea, J. Cernicharo, A. Faure and E. Roueff, *Astrophys. J.*, 2010, **713**, 662.
24 F. J. Aoiz, L. Bañares and V. J. Herrero, *J. Phys. Chem. A*, 2006, **110**, 12546.
25 F. J. Aoiz, V. S. Rábanos, T. González-Lezana and D. E. Manolopoulos, *J. Chem. Phys.*, 2007, **126**, 161101.
26 F. J. Aoiz, T. González-Lezana and V. S. Rábanos, *J. Chem. Phys.*, 2007, **127**, 174109.
27 A. I. Boothroyd, W. J. Keogh, P. G. Martin and M. R. Peterson, *J. Chem. Phys.*, 1996, **104**, 7139.
28 F. R. Ornellas and F. Machado, *J. Chem. Phys.*, 1986, **84**, 1296.
29 F. J. Aoiz, L. Bañares and V. J. Herrero, *J. Chem. Soc., Faraday Trans.*, 1998, **94**, 2483.
30 A. N. Panda, D. Herráez-Aguilar, P. G. Jambrina, J. Aldegunde, S. C. Althorpe and F. J. Aoiz, *Phys. Chem. Chem. Phys.*, 2012, **14**, 13067–13075.
31 P. G. Jambrina, E. Garca, V. J. Herrero, V. Sáez Rábanos and F. J. Aoiz, *J. Chem. Phys.*, 2011, **135**, 03410.
32 L. Bonnet and J.-C. Rayez, *Chem. Phys. Lett.*, 1997, **277**, 183.
33 L. Bonnet and J.-C. Rayez, *Chem. Phys. Lett.*, 2004, **397**, 106.
34 F. J. Aoiz, T. González-Lezana and V. S. Rábanos, *J. Chem. Phys.*, 2008, **129**, 094305.
35 E. J. Rackham, T. González-Lezana and D. E. Manolopoulos, *J. Chem. Phys.*, 2003, **119**, 12895.

